Regular family structures observed in neutron resonance energies: Breathing model of the compound nucleus

Makio Ohkubo
N. Resonance Lab, 1663-39, Senba-cyo, Mito-shi, Ibaraki-ken 310-0851, Japan
(Received 4 May 2012; revised manuscript received 13 August 2012; published 11 January 2013)

In neutron resonances, which are long believed to be a form of quantum chaos, simple regular family structures are found for many even-even nuclei in the several tens of keV to MeV region. Resonance energies can be written by simple arithmetic expressions with good accuracies, where separation energies S_n and G play essential roles and where $G \approx 34.5$ MeV is almost equal to the Fermi energy. Family structures are described for the observed resonances in ^{40}Ca, ^{54}Cr, ^{64}Ni, ^{90}Zr, and ^{208}Pb. Statistical probability tests are performed for the appearance of these family structures. A classical dynamic model of the compound nucleus is proposed where the recurrence of multiple oscillators produces "breathing" and seems to successfully reproduce observed resonance families.

DOI: 10.1103/PhysRevC.87.014608 PACS number(s): 25.40.Ny, 29.30.Hs, 21.10.Dr

I. INTRODUCTION

In classical physics, resonance phenomena always include the time sinusoidal behaviors of physical quantities of the system. Similar situations are found in resonances in many fields of quantum physics and in neutron resonance reactions where an incident neutron excites the compound nucleus (CN). When many oscillators are excited coherently at resonances, they form time-periodic breathing of the CN coherent with the incident neutron wave.

Neutron-nucleus cross sections are essentially important in reactor technology and are widely measured and compiled as basic nuclear data. These cross sections are observed mainly by neutron time-of-flight spectrometers using pulsed accelerator neutron sources. In these cross sections, many sharp resonances (fine structure resonances) are seen for all nuclei as quasistable states of nuclei above neutron separation energies $S_n \sim 8$ MeV. These resonance cross sections are well fitted by the Breit-Wigner formula or the R-matrix formula. Averaged neutron reduced widths are in good agreement with the predictions of the optical model or Ramsauer model. Level densities are very high depending on the target mass number—for example, $\sim$40/MeV for ^{16}O, $\sim$400/MeV for ^{56}Fe, and $\sim 10^5$/MeV for ^{238}U. Each resonance is considered to be a quasistable state of the CN. The CN has a very complicated structure composed of many excited degrees of freedom, and statistical models of the CN work well. In fact, statistical properties of the observed resonances are in good agreement with the predictions of random matrix theory (RMT); the Wigner Gaussian orthogonal ensemble (GOE) distribution for the spacings of nearest neighbor levels of the same J^π, the Porter-Thomas distribution for strengths, and Δ_3 statistics for long-range correlations. Therefore, neutron resonances are thought to be a typical example of quantum chaos [1–4].

However, as is seen in every field of science, different methods of analysis extract different features of the system considered. In fact, many nonrandom properties in observed resonance level positions and spacings have been reported over the past five decades. Using D_{ij} (spacings between two arbitrary levels) distributions and Fourier-like analyses, dominant level spacings are detected which appear more frequently than expected from the random (GOE) distribution of resonance levels [5–12].

Examples of the dominant spacings include, in the eV resonance region, 4.4 eV (^{177}Hf), 5.5 eV (^{123}Sb), 14.6 eV (^{238}U), 17.6 eV (^{168}Er), 142 eV (^{75}As), and 213 eV (^{240}Pu). In the keV or MeV resonance region, spacings are at 460, 515, and 1515 keV (^{16}O), 575 keV (^{32}S), 184 keV (^{40}Ar), 478.4 keV (^{86}Kr), and 86.2 keV (^{140}Ce). These dominant spacings range from several times to several tens of times the average level spacings and were deemed not to be statistical fluctuations but to occur for some physical reason.

Moreover, it is very interesting that simple integer ratios are found among these dominant spacings of different nuclei: 5.5 eV (^{123}Sb)/4.4 eV (^{177}Hf) = 5/4, 14.6 eV (^{238}U)/17.6 eV (^{168}Er) = 5/6, 142 eV (^{75}As)/213 eV (^{240}Pu) = 2/3, etc. in the eV region and 460 keV (^{16}O)/575 keV (^{32}S) = 4/5, 460 keV (^{16}O)/184 keV(^{40}Ar) = 5/2, 575 keV (^{32}S)/478.4 keV (^{86}Kr) = 6/5, 515 keV (^{16}O)/86.2 keV (^{140}Ce) = 6/1, etc. in the keV and MeV region [15] On this subject, detailed descriptions are made by Sukhoruchkin in Ref. [16].

Integer ratios among dominant spacings of different nuclei suggest the existence of a common original energy and spacing over many nuclei. We searched for the original value by repeating least common energies (LCEs) analysis among the dominant spacings of different nuclei, similar to searching for the least common multiple (LCM) among integers. We reached a value $G \approx 34.5$ MeV as the origin of energy and spacing over many nuclei, which is almost equal to the Fermi energy, the maximum energy of the nucleon trapped in the nuclear potential [11]. $G \approx 34.5$ MeV and $\tau_0 = 2\pi\hbar/G = 1.2 \times 10^{-22}$ s play essentially important roles in (quasi)stable states of nuclei under strong interactions.

In this article, excitation energies E_x are expressed as $E_x = (A/B)G$, where A and B are integers and $G \approx 34.5$ MeV. Through this expression, transparent relations are found among E_x, S_n, and E_n, which evoke a semiclassical dynamic model of resonance reactions.

In a previous paper, we reported a recurrence model of the CN where the recurrence times $\tau_{\rm rec}$ for multiple oscillators

are deduced classically by assuming tolerable phase angle errors of 1 rad. Oscillator numbers M excited in the CN are deduced from average level spacings D and E_x for many nuclei. Time behaviors of the CN with periodic recurrences coherent with the incident wave are considered [13]. Simple integer ratios in E_x/S_n are found in many resonances of $^{16}\mathrm{O}+n$. For light nuclei, E_x/S_n values equaling 4/3 and 5/3 appear frequently [14]. For the s-wave resonances of $^{40}\mathrm{Ca}+n$, we found that S_n/E_n values are in the form $17(l/m)$ for many resonances where l, m are small integers. Separation energy $S_n = (17/70)G$ is the sum of two oscillators of $E_1 = (1/7)G$ and $E_2 = (1/10)G$ with recurrence energy $E_{\mathrm{rec}} = (1/70)G = 492$ keV. Many s-wave resonances locate at $E_n = 492(m/l)$ keV [15].

In Sec. II of this article, theoretical descriptions are made on the breathing model and the family structures based on the classical analogy of resonance phenomena. In Sec. III, resonance families are described for the observed resonances in ^{40}Ca, ^{54}Cr, ^{64}Ni, ^{90}Zr, and ^{208}Pb. A discussion is found in Sec. IV, and conclusions are offered in Sec. V.

II. BREATHING MODEL OF THE COMPOUND NUCLEUS

A. Neutron resonances

In classical resonance phenomena, time coherencies are maintained between resonators and the incident waves at resonance frequencies. In neutron resonance reactions, analogous relations will be maintained between the neutron wave frequencies and the oscillation frequencies of the compound nucleus, the Poincaré cycle frequency for multiple oscillators in the CN.

The wave packet length (coherent length) of a slow neutron in the eV region is measured by a neutron interferometer to be $\sim$100 Å $= 10^{-8}$ m, which is very long compared to the nuclear size $\sim 10^{-14}$ m and is formally expressed as a plane wave $\exp[i(\omega t - kx)]$, where the frequency $\omega = E_n/\hbar$, E_n is the neutron kinetic energy, t is time, k is the wave vector, and x is the space coordinate. In crystal diffraction, an incident neutron plane wave is scattered from atoms at periodic lattice points and is diffracted to directions where constructive interference of the scattered wave is maximal. From the diffraction patterns, crystal structures are deduced by Fourier transform. The crystal diffraction is in the (k, x) domain.

In contrast, neutron resonances are in the (ω, t) domain. Time-periodic scattering centers will be produced on the CN surface caused by a change of size or flare-up of neutron density, which is time coherent (synchronized) with the incident wave at resonances. These time behaviors can be deduced from the dispositions of the resonance energies. In the absence of size changes or flare-ups, only the energy-independent potential scattering cross section ($\sim$10 b $= 10 \times 10^{-28}$ m^2) will be observed. Therefore, a dynamic picture of the CN is needed to understand neutron resonances. To this end, we have developed the "breathing model" [13] based on the time-periodic recurrence or flare-up of neutron density on the compound nucleus. This perspective is supported by the S-matrix theory described below.

B. S matrix

An S matrix $S(E)$ is defined for neutron-nucleus reactions from which the cross section $\sigma_s(E) = (\pi/k^2)(2l+1) \mid 1 - S(E) \mid^2$, etc. is determined. A relation between $S(E)$ and the response function is based on Sitenko [17]. For an s-wave resonance, the incident wave $\psi^-(r,t)$ and outgoing wave $\psi^+(r,t)$ around the interaction region of radius R are

$$\psi^-(r,t) = \int_0^\infty dE' a(E')(1/r)\exp[-ik'r - (i/\hbar)E't], \tag{2.1}$$

$$\psi^+(r,t) = \int_0^\infty dE' a(E')S(E')(1/r)\exp[ik'r - (i/\hbar)E't]. \tag{2.2}$$

where $a(E')$ is the amplitude of the incident wave at energy E'. The response function $F(\tau)$ is defined by the causality principle as

$$\psi^+(r,t) = \int_0^\infty d\tau F(\tau)\psi^-(r, t-\tau). \tag{2.3}$$

By multiplying Eqs. (2.1), (2.2), and (2.3) by $\exp(-iEt/\hbar)$ and integrating over t from $-\infty$ to ∞, $S(E)$ can be expressed as a Fourier transform of the response function $F(\tau)$ as

$$S(E)e^{2ikR} = \int_0^\infty d\tau F(\tau)e^{i\frac{E\tau}{\hbar}}, \tag{2.4}$$

where τ is the time for the response to return.

Equation (2.4) is a basic relation on which the following discussions are based. In the continuum region, $S(E)$ has no peak, and $F(\tau)$ is expected to be a nonperiodic or stochastic function of an infinitely long time period. In contrast, for an isolated resonance at E_0, $S(E)$ has a peak at E_0 (recoil corrected). That is, the scattered wave $\psi^+(r,t)$ is significant if $F(\tau)$ and the incident wave $\psi^-(r,t)$ are time coherent with each other, during the lifetime $\sim h/\Gamma$, where Γ is the total width of the resonance. Off resonance, only potential scattering remains. At resonance, $F(\tau)$ must be a periodic function with a period $\tau_{\mathrm{rec}} = 2\pi\hbar/E_0$, or, more generally, $\tau_{\mathrm{rec}} = (l/m)(2\pi\hbar/E_0)$, where l, m are small integers.

C. Requirement of time periodicity for the normal modes

At resonance, the response function $F(\tau)$ can be expressed by a Fourier series with higher harmonics of periods $\tau_j = \tau_{\mathrm{rec}}/k_j$ and frequencies $\omega_j = k_j(l/m)E_0/\hbar$, where k_j are integers ($j = 1, 2, \ldots, M$), with M the number of harmonics, which are considered to be equivalent to the degrees of freedom excited at resonance. Frequency ratios as well as time periods of these higher harmonics are commensurable (forming integer ratios) with each other. A unit time $\tau_0 = 1.20 \times 10^{-22}$ s exists as the greatest common divisor (GCD) of τ_j ($j: 1, 2, \ldots, M$), and τ_j is quantized as $n_j\tau_0$ where n_j is an integer. The recurrence time τ_{rec} is the least common multiple for the ensemble $(n_j; j = 1, 2, \ldots, M)$ multiplied by τ_0. The frequency component ω_j is proportional to the inverse integers $\omega_j = (2\pi/\tau_0)/n_j = (1/\hbar)G/n_j$. These higher

harmonics are equivalent to the normal modes excited on the CN at resonances.

Though the details are not known, the Hamiltonian and wave functions for these normal modes are formally written as

$$H = H_1 + H_2 + \cdots + H_M, \tag{2.5a}$$

$$\psi(x,t) = \psi_1(x_1,t) \otimes \psi_2(x_2,t) \cdots \otimes \psi_M(x_M,t). \tag{2.5b}$$

The time periodic conditions are

$$\psi_j(x_j,t) = \psi_j(x_j, t + n_J \tau_0), \tag{2.6a}$$

$$\psi(x,t) = \psi(x, t + \tau_{\rm rec}), \tag{2.6b}$$

where

$$\tau_{\rm rec} = {\rm LCM}(n_1, \ldots, n_M)\tau_0. \tag{2.6c}$$

The total excitation energy $E_x = S_n + E_0$ for these normal modes,

$$E_x = \hbar(\omega_1 + \omega_2 + \cdots + \omega_M), \tag{2.7a}$$

is rewritten as

$$E_x = \frac{2\pi\hbar}{\tau_0} \sum_{j=1}^{M} \frac{1}{n_j} = G \sum_{j=1}^{M} \frac{1}{n_j} \quad (n_j : \text{integer}). \tag{2.7b}$$

For multiple excitations, the ones in the numerators in (2.7b) will be replaced by small integers a_j.

D. Resonance energy

There are many cases shown in Sec. III where the separation energies S_n are the sum of q oscillators, where $q = M - 1$,

$$S_n = G \sum_{j=1}^{q} \frac{1}{n_j}, \tag{2.8}$$

with recurrence time $\tau_{\rm rec} = {\rm LCM}(n_1, \ldots, n_q)\tau_0$. Analogous to the classical resonance phenomena, neutron resonance reactions take place when the time periods of the neutron wave τ_w are simple integer ratios (m/l) to $\tau_{\rm rec}$, i.e.,

$$\tau_w = \left(\frac{l}{m}\right)\tau_{\rm rec} = \left(\frac{l}{m}\right){\rm LCM}(n_1, \ldots, n_q)\tau_0, \tag{2.9a}$$

that is,

$$E_n = E_{\rm rec}\left(\frac{m}{l}\right). \tag{2.9b}$$

This is a kind of Fermi resonance (described in Sec. IV) where the recurrence energy $E_{\rm rec}$ of the CN is defined as

$$E_{\rm rec} = \frac{2\pi\hbar}{{\rm LCM}(n_1, \ldots, n_q)\tau_0} = \frac{G}{{\rm LCM}(n_1, \ldots, n_q)}. \tag{2.10}$$

For incident neutron energies of $E_{\rm rec}(m/l)$, the recurrence of (CN + neutron wave) takes place every $l \times \tau_{\rm rec}$. For two oscillators $q = 2$, ${\rm LCM}(n_1, n_2) = n_1 n_2$ (irreducible case), and S_n is

$$S_n = \left(\frac{1}{n_1} + \frac{1}{n_2}\right)G, \tag{2.11}$$

and $E_{\rm rec}$ is

$$E_{\rm rec} = \frac{G}{n_1 n_2} = \frac{S_n}{n_1 + n_2}. \tag{2.12}$$

Then

$$E_n = E_{\rm rec}\left(\frac{m}{l}\right) \ (l, m : \text{small integers}), \tag{2.13}$$

$$E_x = S_n + E_n = \left[\left(\frac{1}{n_1} + \frac{1}{n_2}\right) + \frac{1}{n_1 n_2}\frac{m}{l}\right]G = \left[1 + \frac{1}{n_1 + n_2}\frac{m}{l}\right]S_n. \tag{2.14}$$

These relations are valid for many observed resonances of small l, m composing a family as described in Sec. III.

E. Dynamic behaviors of the compound nucleus

The breathing model is developed as a mechanism of the neutron resonance reaction and is outlined below. A neutron wave incident on a target nucleus is divided into two components: (1) a pass-by component that passes by without interaction and (2) a penetrating component which excites q oscillators (normal modes) in the CN simultaneously. The observed cross section is the result of (1) and (2). The separation energy is divided into q oscillators in the form $S_n = G\sum_{j=1}^{q}(1/n_j)$. These oscillators will be fast deformations (phonon) or particles in orbit or other oscillations with cycle times quantized by unit time $\tau_0 = 1.20 \times 10^{-22}$ s. The recurrence time of the CN is $\tau_{\rm rec} = {\rm LCM}(n_1, \ldots, n_q)\tau_0$. The response function $F(\tau)$ behaves like a pulse array with a pulse separation $\tau_{\rm rec}$ with intermittent pulses like breathing of the CN, making scattering centers on the time axis. Resonance reactions take place for the case $\tau_w = (l/m)\tau_{\rm rec}$. The breathing frequency (equivalent to the recurrence frequency) depends on the LCM, which is a complicated function of E_x as described in Sec. III. The envelope of the pulse array decays exponentially with the time constant $\hbar/\Gamma$, where Γ is a fine structure level width.

For the physical meaning of (m/l), the stroboscopic analogy described in Sec. IV is plausible.

At every $\tau_{\rm rec}$, the penetrating component reverts to the initial phase, gathers to form a high neutron-density flare on the CN surface, and interferes with the pass-by component. The nuclear potential deformation is maximized so that the neutron wave penetrates easily through the nuclear surface. The instance of the recurrence ($\Delta_g \sim$ a few τ_0) is called the coalescent phase in [13], or the gather phase in [14], and is analogous to a time slit which opens to allow interference between the two components during Δ_g at every $\tau_{\rm rec}$. Energy spectra expected from these time structures are almost consistent with the observed facts [13], are equidistant fine structure resonances of width Γ and level spacing $D = 2\pi\hbar/\tau_{\rm rec}$, and are enveloping giant resonances of width Γ_G corresponding to the opening durations, i.e., $\Gamma_G \sim 2\pi\hbar/\Delta_g \sim 10$ MeV. Also spatial distributions of wave functions will be related to J^π and strengths for each resonances. Further discussions are in Sec. IV and Fig. 4.

III. REGULAR FAMILY STRUCTURES IN NEUTRON RESONANCES OF EVEN-EVEN TARGET NUCLEI

In this section, we show family structures on the observed s-wave neutron resonances in ^{40}Ca, ^{54}Cr, ^{64}Ni, ^{90}Zr, and ^{208}Pb. S-wave resonances have generally large Γ_n values and are thought to be caused by relatively simple reaction mechanisms. Average level spacings of these nuclei are fairly large, which is important for this analyses. The probabilities of appearance for these family structures are calculated on the assumptions described below. In many cases, several families of Groups (I) and (II) coexist and overlap. Classification of resonances into several groups can be made by $E_{\rm rec}$, which is determined as described below. Though somewhat tedious, we will show detailed numerical data to support our viewpoint.

A. Assumptions on statistical tests

In order to assert family structures (patterns) among the level sequences, probabilities of appearance of the patterns P_s are very important. If the calculated P_s for a pattern A is in the several tens of percent range, the pattern A almost always appears and has no special meaning. If the P_s for a pattern B is less than a few percent, the appearance of pattern B is a rare event and is considered to be caused by some physical reason.

The problem here is to estimate the probability of appearance of the family structures: n_l levels disposed in the region R and n_s levels out of n_l are on the special points at $(m/l)E_{\rm rec}$ within total deviation widths ϵ, where $(l, m \leqslant 10)$.

For the n_l levels, an RMT ensemble must be used for this case. The Wigner (GOE) distribution for the nearest neighbor level spacings, next-nearest neighbor distribution, next-next-nearest one, ... are given by complicated formulas. The sum of these distribution functions is a constant value for a large sequence of levels. However, exact probability calculations for the RMT ensembles are very difficult for these family structures.

Therefore, we substitute random (homogeneous) level ensembles where probabilities of appearance are given by binomial distributions. For a distance larger than the average spacing, small differences are expected between the two. The probabilities of appearance summarized in Table II are estimated for random ensembles which are good approximations for RMT ensembles.

B. Search for $E_{\rm rec}$ in resonance energies

The recurrence energy $E_{\rm rec}$ values of a CN at resonances are essential for the breathing model. To read out $E_{\rm rec}$ among observed resonances, we use three methods: (1) Search for a common factor α in the integer ratios S_n/E_n for many resonances. For example, factor 17 in ^{40}Ca(I) is shown in Table I. $E_{\rm rec}$ is S_n/α. (2) Search for a simple integer ratio in $S_n/G = \alpha/\beta$ where $G \sim 34.5$ MeV; for example, $S_n/G = 17/70$ in ^{40}Ca(I) where $G = 34434$ keV. (3) Search for a pair of resonances E_1, E_2 whose energy ratios are a simple integer ratio belonging to the same family. That is,

$$E_1 = (m_1/l_1)E_{\rm rec}, \quad E_2 = (m_2/l_2)E_{\rm rec} \tag{3.1}$$

and the ratio is

$$\frac{E_2}{E_1} = \frac{m_2 l_1}{m_1 l_2}. \tag{3.2}$$

The LCE is given as

$$\text{LCE} = E_1 m_2 l_1 = E_2 m_1 l_2 = m_1 m_2 E_{\rm rec}, \tag{3.3}$$

which is an integer multiple of $E_{\rm rec}$. S_n/LCE is an integer divisor of the common factor α:

$$\frac{S_n}{\text{LCE}} = \frac{1}{m_1 m_2}\frac{S_n}{E_{\rm rec}} = \frac{\alpha}{m_1 m_2}. \tag{3.4}$$

The spectrum S_n/LCE for many pairs of levels shows α visually.

By complementary use of these methods, $E_{\rm rec}$ can be derived. For the sake of convenience, integer multiples or divisors of $E_{\rm rec}$ are used depending on the case.

C. ^{40}Ca(I) s-wave resonances

The original resonance data of $^{40}\text{Ca} + n$ are from Toepke [18], where 40 s-wave resonances below $E_n \leqslant 2.4$ MeV are reported. The separation energy is $S_n = 8362.7$ keV. The cumulative number of levels versus neutron energy is shown in Fig. 1(a), and the nearest neighbor level spacing distribution is shown in Fig. 1(b) with a Wigner distribution. In Fig. 2, $g\Gamma_n$ values versus neutron energy are shown, where classifications to Groups (I) and (II) are made. Numerical data for the 40 resonances, E_n, $g\Gamma_n$, S_n/E_n, $= S_n/E_n$, Group, m/l, $E^1_{\rm rec}(m/l)$, $E^2_{\rm rec}(m/l)$, and δ are shown in Table I, where $E^1_{\rm rec}$ and $E^2_{\rm rec}$ means $E_{\rm rec}$ for Groups (I) and (II), respectively.

In Figs. 1(a) and 1(b), common statistical features are seen for this nucleus. As described in the introduction, we have remarked on the frequent appearance of the factor 17 as $S_n/E_n = 17(l/m)$, where l, m are small integers [Group (I)] [15]. The existence of these special structures $[E_n = (m/l)(1/17)S_n]$ seems to have no effect on the statistical distributions in Figs. 1(a) and 1(b).

Moreover, it is very interesting that the separation energy $S_n = 8362.7$ keV can be expressed as $(17/70)G$, which can be rewritten as $(1/7 + 1/10)G$ with $G = 34434$ keV. This corresponds to two oscillators of cycle time $7\tau_0$ and $10\tau_0$, and with recurrence time $\text{LCM}(7, 10)\tau_0 = 70\tau_0$. The recurrence energy is $E^1_{\rm rec} = (1/70)G = (1/17)S_n = 491.9$ keV. The observed resonances E_n dispose nearby calculated energies $E^c_n = 491.9(m/l)$ keV with deviation δ, as shown in Table I. These resonances are called the "492 keV family." ^{40}Ca(I) is a typical example of the breathing model.

Arithmetic relationships for ^{40}Ca(I) are as follows (where $n_1 = 7$ and $n_2 = 10$):

$$S_n = 8362.7 \text{ keV} = \frac{17}{70}G = \left(\frac{1}{7} + \frac{1}{10}\right)G, \quad G = 34434 \text{ keV}, \tag{3.5}$$

$$E^1_{\rm rec} = \frac{G}{70} = \frac{S_n}{17} = 491.9 \text{ keV}, \quad {}^{40}\text{Ca(I)}, \tag{3.6}$$

TABLE I. $^{40}\mathrm{Ca}+n$ S-wave resonances. Group (I): $S_n = 8362.7$ keV $= (17/70)G = (1/7 + 1/10)G$, $G = 34434$ keV, $E^1_{\mathrm{rec}} = G/70 = S_n/17 = 491.9$ keV. Group (II): $S_n = 8362.7$ keV $= (39/162)G = (1/6 + 1/18 + 1/54)G$, $G = 34737$ keV, $E^2_{\mathrm{rec}} = G/162 = S_n/39 = 214.4$ keV, $\delta = E_n - (m/l)E_{\mathrm{rec}}$.

j	E_n (keV)	$g\Gamma_n$ (keV)	S_n/E_n	$=S_n/E_n$	Group	m/l	$492(m/l)$ (keV)	$214(m/l)$ (keV)	δ (keV)
1	86.8	0.14	390/4	$39\times5/2$	II	2/5		85.8	1.0
2	128.6	3.3	65/1	$39\times5/3$	II	3/5		128.6	0.0
3	164.4	2.5	51/1	$17\times3/1$	I	1/3	163.9		0.5
4	211.2	7.4	119/3	$17\times7/3$	I	3/7	210.8		0.4
			39/1	$39\times1/1$	II	1/1		214.4	−3.2
5	244.8	20	34/1	$17\times2/1$	I	1/2	245.9		−1.2
			273/8	$39\times7/8$	II	8/7		245.0	−0.3
6	283.8	2	117/4	$39\times3/4$	II	4/3		285.9	−2.1
7	319.9	14	26/1	$39\times2/3$	II	3/2		321.6	−1.7
8	346.2	1.8	170/7	$17\times10/7$	I	7/10	344.3		1.9
			195/8	$39\times5/8$	II	8/5		343.1	2.7
9	376.5	0.5	156/7	$39\times4/7$	II	7/4		375.2	1.3
10	437.3	10	153/8	$17\times9/8$	I	8/9	437.2		0.1
11	494.5	10	17/1	$17\times1/1$	I	1/1	491.9		2.6
12	545.2	1.1	153/10	$17\times9/10$	I	10/9	546.6		−1.4
13	576.4	55	102/7	$17\times6/7$	I	7/6	573.9		2.5
14	619.8	2	68/5	$17\times4/5$	I	5/4	614.9		4.9
15	658.4	2.7	51/4	$17\times3/4$	I	4/3	655.9		2.5
16	720.0	3.2	221/19	$17\times13/19$	I	19/13	719.0		1.0
17	724.5	4.4	104/9	$39\times8/27$	II	27/8		723.7	0.8
18	752.5	12	78/7	$39\times2/7$	II	7/2		750.5	2.0
19	773.0	2.4	65/6	$39\times5/18$	II	18/5		771.9	1.1
20	802.7	3.5	52/5	$39\times4/15$	II	15/4		804.1	−1.4
21	840.6	29	119/12	$17\times7/12$	I	12/7	843.3		−2.7
22	857.0	31	68/7	$17\times4/7$	I	7/4	860.9		−3.9
			39/4	$39\times1/4$	II	4/1		857.7	−0.7
23	946.1	7.2	221/25	$17\times13/25$	I	25/13	946.0		0.1
			195/22	$39\times5/22$	II	22/5		943.5	2.6
24	979.2	12	17/2	$17\times1/2$	I	2/1	983.8		−4.6
25	1067.9	12	102/13	$17\times6/13$	I	13/6	1065.8		2.1
			39/5	$39\times1/5$	II	5/1		1072.1	−4.2
26	1181.0	12	85/12	$17\times5/12$	I	12/5	1180.6		0.4
			78/11	$39\times2/11$	II	11/2		1179.4	1.6
27	1252.4	12	260/39	$39\times20/117$	II	117/20		1254.4	−2.0
			260/39	$39\times6/35$	II	35/6		1250.8	1.6
28	1285.7	4	13/2	$39\times1/6$	II	6/1		1286.6	−0.9
29	1341.1	3.8	156/25	$39\times4/25$	II	25/4		1340.2	0.9
30	1478.7	2	17/3	$17\times1/3$	I	3/1	1475.8		2.9
31	1558.2	3.4	102/19	$17\times6/19$	I	19/6	1557.8		0.4
32	1593.0	4.3	68/13	$17\times4/13$	I	13/4	1598.8		−5.8
33	1609.4	30	26/5	$39\times2/15$	II	15/2		1608.2	1.2
34	1684.2	4.2	104/21	$17\times7/24$	I	24/7	1686.6		−2.4
35	1748.0	4	153/32	$17\times9/32$	I	32/9	1749.0		1.1
36	1855.1	16	117/26	$39\times3/26$	II	26/3		1858.4	−3.3
37	1975.1	20	17/4	$17\times1/4$	I	4/1	1967.7		7.4
38	2129.2	14	51/13	$17\times3/13$	I	13/3	2131.7		−2.7
39	2219.0	30	34/9	$17\times2/9$	I	9/2	2213.7		5.3
40	2370.1	20							

$$E^c_n = E^1_{\mathrm{rec}}\left(\frac{m}{l}\right) = 491.9\left(\frac{m}{l}\right)\ \mathrm{keV} \quad (l, m : \text{small integers}), \tag{3.7}$$

$$\frac{S_n}{E^c_n} = (n_1 + n_2)\left(\frac{l}{m}\right) = 17\left(\frac{l}{m}\right), \quad {}^{40}\mathrm{Ca(I)}. \tag{3.8}$$

The deviation δ for the observed resonance energy E_n is defined as

$$\delta = E_n - E^c_n. \tag{3.9}$$

Among the 40 s-wave resonances below $E_n \leqslant 2.4$ MeV, 15 are at $E_n = 491.9(m/l)$ keV with ($l,\ m \leqslant 10$), where (m/l)

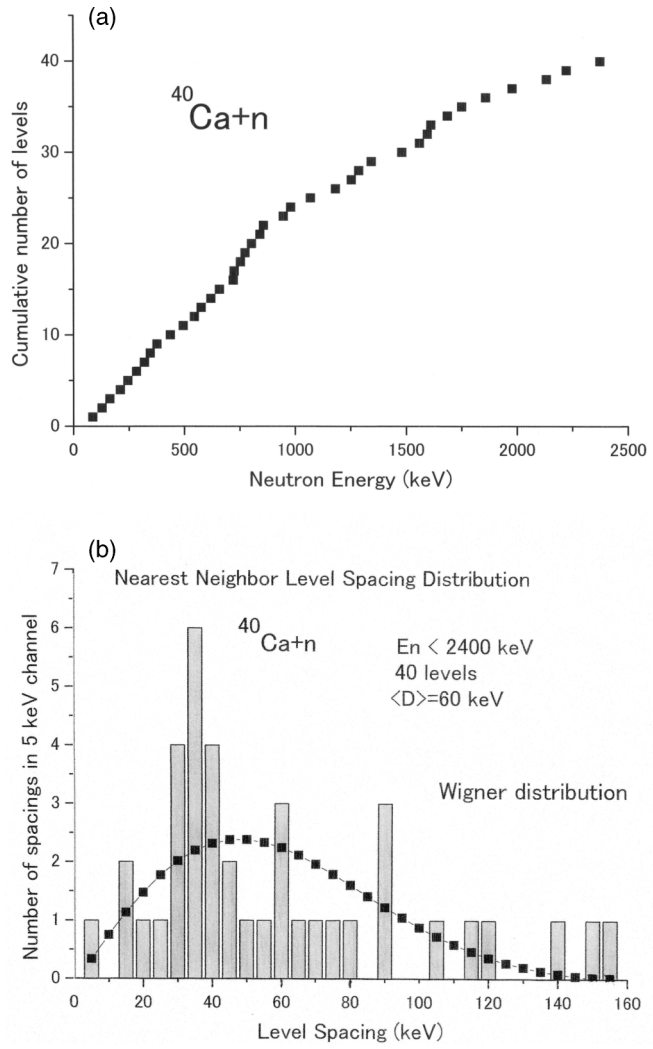

FIG. 1. (a) Cumulative number of s-wave resonance levels vs neutron energy. (b) Nearest neighbor level spacing distribution with a Wigner distribution.

are 1/3, 3/7, 1/2, 7/10, 8/9, 1/1, 10/9, 7/6, 5/4, 4/3, 7/4, 2/1, 3/1, 4/1, and 9/2, with small δ.

Of course, any values of E_n can be fitted using large numbers of l, m, but these have no physical meaning. Since small integers in l, m are physically important, we restrict $l, m \leqslant 10$.

The statistical probabilities of appearance are calculated for the pseudofamily of Group (I) by assuming random dispositions of the $n_l = 40$ levels in the energy region from 70 to 2400 keV. Deviations of observed E_n from calculated values $E_{\rm rec}(m/l)$ are within a width of $\epsilon = 5$ keV for $n_s = 10$ levels. Candidate cases (m/l) $(l, m \leqslant 10)$ are carefully counted in the (l, m) plane to be $B = 53$, where (2,2), (2,4), . . ., (3,3), (3,6), . . . are inhibited to prevent double counting. For a level placed at random in the region ($R = 2330$ keV), the probability of being an integer ratio is $p = (\epsilon B)/R = 0.114$. For 40 levels placed at random, the expected number of levels of integer ratios is $n_l p = 4.6$. The probability for 10 levels out of 40 being integer ratios is calculated by the binomial distribution: $P_r(10, 40, p) = {}_{40}\mathrm{C}_{10}\ p^{10}(1-p)^{30} \approx 0.0083 = 0.83\%$, and the sum $P_s = \sum_{j=10}^{40} P_r(j, 40, p) \leqslant 1.2\%$. Similar calculations are made for the low-energy region from 70 to 1000 keV, where $n_l = 24$ and $n_s = 9$ with $\epsilon = 4$ keV. The probability of appearance of the family is calculated to be $P_s \leqslant 2.6\%$. Numerical data for probability calculations are summarized in Table II.

D. ^{40}Ca(II) s-wave resonances

In s-wave resonances of $^{40}\mathrm{Ca} + n$, there are several resonances which do not belong to Group (I) and show $S_n/E_n = 13(l/m)$ [Group (II)]. $S_n = 8362.7$ keV is alternatively expressed as $S_n = (13/54)G$ with $G = 34737$ keV, which is decomposed into a sum of inverse integers as

$$S_n = \frac{13}{54}G = \frac{39}{162}G = \left(\frac{1}{6} + \frac{1}{18} + \frac{1}{54}\right)G, \quad G = 34737\ \text{keV}, \quad {}^{40}\mathrm{Ca(II)}. \tag{3.10}$$

The recurrence energy $E^2_{\rm rec} = G/162 = S_n/39 = 214.4$ keV is used. Resonance energies of the 214 keV family are expressed as

$$E^c_n = \frac{1}{162}\left(\frac{m}{l}\right)G = \frac{1}{39}\left(\frac{m}{l}\right)S_n = 214.4\left(\frac{m}{l}\right)\ \text{keV}, \quad {}^{40}\mathrm{Ca(II)}. \tag{3.11}$$

The lowest two s-wave resonances observed at $E_n = 86.8$ and 128.6 keV are regarded as $m/l = 2/5$ and 3/5, respectively, with good accuracies with $\delta \sim 1$ keV. Twelve s-wave resonances below 2400 keV are at $E_n = 214.4(m/l)S_n$, where (m/l) for $(l, m \leqslant 10)$ are 2/5, 3/5, 1/1, 8/7, 4/3, 3/2, 8/5, 7/4, 7/2, 4/1, 5/1, and 6/1 with deviations $|\delta| \leqslant 4.2$ keV. Resonances at 211, 245, 346, 857, 946, 1067, 1181, and 1252 keV belong together to Groups (I) and (II). A resonance at $E_n = 376$ keV was first classified in Group (I) with $\delta = 7.0$ keV [15], but it seems reasonable to classify it in Group (II) with $m/l = 7/4$ and $\delta = 1.3$ keV. Numerical data for the probability calculations are summarized in Table II.

E. ^{54}Cr(I) s-wave resonances

The original data for $^{54}\mathrm{Cr} + n$ resonances are from Carlton *et al.* [19]. Fifty-four s-wave resonances are observed in $E_n \leqslant 2$ MeV as shown in Tables III and IV. $g\Gamma_n$ values versus E_n are shown in Fig. 3. In the integer ratios S_n/E_n, two types predominate: $16(m/l)$ Group (I) and $9(m/l)$ Group (II). It is interesting that most of the large $g\Gamma_n$ resonances belong to Group (I). For Group (I), $S_n = 6246.3$ keV is regarded as

$$S_n = 6246.3\ \text{keV} = \frac{2}{11}G = \frac{16}{88}G = \left(\frac{1}{8} + \frac{1}{22} + \frac{1}{88}\right)G, \quad G = 34354\ \text{keV}, \quad {}^{54}\mathrm{Cr(I)}, \tag{3.12}$$

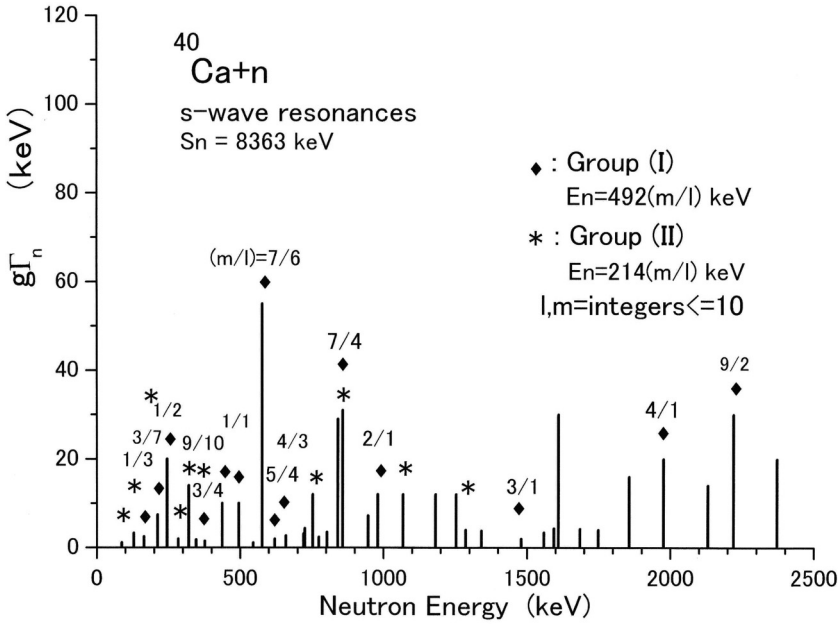

FIG. 2. S-wave resonances of $^{40}\mathrm{Ca}+n$ below 2400 keV. Groups (I) and (II) are shown.

with LCM = 88 and $E^1_{\mathrm{rec}} = G/88 = S_n/16 = 390.4$ keV. A large s-wave resonance at $E_n = 585.4$ keV is $(3/2)E^1_{\mathrm{rec}}$ with a deviation of less than 1 keV. Thirteen resonances including $E_n = 585.4$ keV are at $E_n = 390.4(m/l)$ keV as shown in Tables III and IV, where (m/l) are 3/10, 1/3, 4/9, 5/7, 8/9, 10/7, 3/2, 5/3, 2/1, 5/2, 8/3, 7/2, and 5/1 for $(l, m \leqslant 10)$ and with deviations $|\delta| \leqslant 1$ keV except 2/1 (778 keV), 5/2 (985 keV), and 8/3 (1046 keV). Among the energies of large resonances in Group (I), simple multiple integer ratios are found; $1463/585 = 5/2, 1952/585 = 10/3, 1824/1140 = 8/5$, etc. E^c_n can be expressed as

$$E^c_n = \frac{1}{88}\left(\frac{m}{l}\right)G = \frac{1}{16}\left(\frac{m}{l}\right)S_n = 390.4\left(\frac{m}{l}\right)\ \text{keV}, \quad {}^{54}\mathrm{Cr(I)}. \tag{3.13}$$

Numerical data for the probability calculations are summarized in Table II.

F. ^{54}Cr(II) s-wave resonances

For Group (II), S_n/E_n ratios are of the type $9(m/l)$. S_n is alternatively expressed as

$$S_n = 6246.3\ \text{keV} = \frac{9}{50}G = \left(\frac{1}{10}+\frac{2}{25}\right)G, \quad G = 34701\ \text{keV}, \quad {}^{54}\mathrm{Cr(II)}, \tag{3.14}$$

with LCM = 50 and $E^2_{\mathrm{rec}} = G/50 = S_n/9 = 694.0$ keV. Many small resonances belong to Group (II) with energies at $E^c_n = E^2_{\mathrm{rec}}(m/l)$, where (m/l) are 1/4, 2/5, 1/2, 4/5, 9/8, 5/4, 9/7, 4/3, and 9/5 with $(l, m \leqslant 10)$ and with deviations $\delta \leqslant 2.5$ keV as shown in Tables III and IV. For resonances of 3/2, 8/5, 7/4, and 5/2, δ values are larger. E^c_n can be expressed as

$$E^c_n = \frac{1}{50}\left(\frac{m}{l}\right)G = \frac{1}{9}\left(\frac{m}{l}\right)S_n = 694.0\left(\frac{m}{l}\right)\ \text{keV}, \quad {}^{54}\mathrm{Cr(II)}. \tag{3.15}$$

TABLE II. Numerical data for probability calculations. R: Energy region, n_l: total number of levels, n_s: number of levels being (m/l) within ϵ, L: maximum of m, l, B: number of possible points (m/l) $(m, l \leqslant L)$, ϵ: total deviation width, p: probability for a random point to be in the candidate region, P_s: probability of being in the candidate region for more than n_s random points out of n_l.

Z	Target nucleus	Group	Region R (keV)	n_l	n_s	L	B	ϵ (keV)	$p = \epsilon B/R$	P_s (%)
20	Ca-40	(I)	2330	40	10	10	53	5.0	0.114	1.2
		(I)	930	24	9	10	44	4.0	0.189	2.6
		(II)	2330	40	9	10	53	4.1	0.093	1.1
24	Cr-54	(I)	2000	54	10	10	58	2.0	0.058	0.10
		(II)	1000	24	8	10	42	4.7	0.197	8.1
28	Ni-64		580	27	9	10	24	3.4	0.140	1.0
40	Zr-90	(A)	300	27	9	10	44	1.1	0.161	2.1
		(B)	300	22	8	10	44	1.0	0.146	1.0
82	Pb-208		1750	4	4	10	40	13.4	0.304	–

TABLE III. $^{54}\mathrm{Cr}+n$ s-wave resonances, $S_n = 6246.3$ keV. Group (I): $S_n = (16/88)G = (1/8 + 1/22 + 1/88)G$, $E_{\mathrm{rec}} = S_n/16 = 390.4$ keV, $E_n = 390.4(m/l)$ keV, $G = 34354$ keV. Group (II): $S_n = (9/50)G = (1/10 + 2/25)G$, $E_{\mathrm{rec}} = S_n/9 = 694.0$ keV, $E_n = 694.0(m/l)$ keV, $G = 34701$ keV. Several resonances belong to both groups.

j	E_n (keV)	$g\Gamma_n$ (keV)	S_n/E_n	$= S_n/E_n$	Group	m/l	$390(m/l)$ (keV)	$694(m/l)$ (keV)	δ (keV)
1	22.6	0.6	3600/13	$9\times400/13$	II	13/400		22.5	0.1
2	117.0	5.0	160/3	$16\times10/3$	I	3/10	117.1		−0.1
3	129.0	0.3	48/1	$16\times3/1$	I	1/3	130.1		−1.1
4	173.2	2.0	36/1	$16\times9/4$	I	4/9	173.5		−0.3
				$9\times4/1$	II	1/4		173.5	−0.3
5	278.2	11.1	112/5	$16\times7/5$	I	5/7	278.8		−0.6
			45/2	$9\times5/2$	II	2/5		277.6	0.6
6	323.5	12.3	135/7	$9\times15/7$	II	7/15		323.8	−0.3
7	346.3	0.44	18/1	$16\times9/8$	I	8/9	347.0		−0.7
				$9\times2/1$	II	1/2		347.0	−0.7
8	426.4	12.0	117/8	$9\times13/8$	II	8/13		427.1	−0.7
9	478.6	18.1	13/1	$9\times13/9$	II	9/13		480.5	−1.9
10	557.4	0.5	112/10	$16\times7/10$	I	10/7	557.7		−0.3
			45/4	$9\times5/4$	II	4/5		555.2	2.2
11	585.3	102	32/3	$16\times2/3$	I	3/2	585.6		−0.3
12	650.9	3.9	144/15	$16\times9/15$	I	5/3	650.6		0.3
				$9\times16/15$	II	15/16		650.6	0.3
13	655.2	2.1	162/17	$9\times18/17$	II	17/18		655.5	−0.3
14	727.4		180/21	$9\times20/21$	II	21/20		728.7	−1.3
15	740.0	5.2	135/16	$9\times15/16$	II	16/15		740.3	−0.3
16	778.4	0.1	8/1	$16\times1/2$	I	2/1	780.8		−2.4
				$9\times8/9$	II	9/8		780.8	−2.4
17	796.7	0.4	117/15	$9\times13/15$	II	15/13		800.8	−4.1
18	865.0	0.1	36/5	$16\times9/20$	I	20/9	867.5		−2.5
				$9\times4/5$	II	5/4		867.5	−2.5
19	873.5	1.1	50/7	$9\times50/63$	II	63/50		874.5	−1.0
20	886.2	0.2	360/51	$9\times40/51$	II	51/40		884.9	1.3
21	891.3	3.0	7/1	$16\times7/16$	I	16/7	892.3		−1.0
				$9\times7/9$	II	9/7		892.3	−1.0
22	898.8	0.2	90/13	$9\times10/13$	II	13/10		902.2	−3.4
23	924.3	0.3	27/4	$9\times3/4$	II	4/3		925.3	−1.0
24	943.3	1.0	126/19	$9\times14/19$	II	19/14		941.9	1.4
25	959.7	10.6	13/2	$9\times13/18$	II	18/13		960.9	−1.2
26	985.5	38.3	32/5	$16\times2/5$	I	5/2	975.9		9.6
27	1018.4	26	80/13	$16\times5/13$	I	13/5	1015.0		3.4
28	1046.3	0.5	6/1	$16\times3/8$	I	8/3	1041.0		5.3
				$9\times2/3$	II	3/2		1041.0	5.3
29	1071.6	0.3	64/11	$16\times4/11$	I	11/4	1073.5		−1.9
30	1087.2	0.2	63/11	$9\times7/11$	II	11/7		1090.6	−3.4
31	1096.6	2.4	108/19	$9\times12/19$	II	19/12		1098.8	−2.2
32	1119.4	0.3	45/8	$9\times5/8$	II	8/5		1110.4	9.0
33	1140.0	55	192/35	$16\times12/35$	I	35/12	1138.6		1.4
34	1208.8	6.6	36/7	$9\times4/7$	II	7/4		1214.5	−5.7
35	1250.6	0.2	5/1	$16\times5/16$	I	16/5	1249.2		1.4
				$9\times5/9$	II	9/5		1249.2	1.4

Numerical data for the probability calculations are summarized in Table II.

G. ^{64}Ni s-wave resonances

In $^{64}\mathrm{Ni}+n$, 27 s-wave resonances were observed by Beer *et al.* [20] and Farrell *et al.* [21] below $E_n \leqslant 580$ keV as shown in Table V. Though the data are out of date, we found the frequent appearance of the factor 8 in the integer ratios S_n/E_n. $S_n = 6098.0$ keV is regarded as

$$S_n = 6098.0\ \mathrm{keV} = \frac{8}{45}G = \left(\frac{1}{9}+\frac{1}{15}\right)G, \qquad G = 34301\ \mathrm{keV}, \quad {}^{64}\mathrm{Ni}, \tag{3.16}$$

with LCM = 45 and $E_{\mathrm{rec}} = G/45 = S_n/8 = 762.2$ keV. Nine s-wave resonances are at $E_n^c = 762.2(m/l)$ keV, where (m/l) are 1/6, 1/5, 3/10, 2/5, 3/7, 1/2, 5/8, 5/7, and 3/4 with

TABLE IV. ^{54}Cr + n s-wave resonances *(Continued.)*.

j	E_n (keV)	$g\Gamma_n$ (keV)	S_n/E_n	$= S_n/E_n$	Group	m/l	$390(m/l)$ (keV)	$694(m/l)$ (keV)	δ (keV)
36	1281.8	5.6	81/14	$9 \times 9/14$	II	14/9		1079.5	2.3
37	1344.3	14.2	14 /3	$9 \times 14/27$	II	27/14		1338.5	5.8
38	1366.9	0.3	32/7	$16 \times 2/7$	I	7/2	1366.3		0.6
39	1402.7	0.7	40/9	$16 \times 5/18$	I	18/5	1405.4		−2.4
40	1407.7	1.9	40/9	$16 \times 5/18$	I	18/5	1405.4		2.3
41	1421.4	0.4	180/41	$9 \times 20/41$	II	41/20		1422.7	−1.3
42	1426.3	0.9	153/35	$9 \times 17/35$	II	35/17		1428.9	−2.6
43	1463.6	25	64/15	$16 \times 4/15$	I	15/4	1463.9		−0.3
44	1482.3	0.7	63/15	$9 \times 7/15$	II	15/7		1487.2	−4.9
45	1495.0	1.1	63/15	$9 \times 7/15$	II	15/7		1487.2	7.8
46	1533.3	1.3	45/11	$9 \times 5/11$	II	11/5		1526.8	6.5
47	1686.4	1.6	63/17	$9 \times 7/17$	II	17/7		1685.5	0.9
48	1731.6	4.8	18/5	$9 \times 2/5$	II	5/2		1735.0	−3.4
49	1761.0	4.0	117/33	$9 \times 13/33$	II	33/13		1761.7	−0.7
50	1767.9	1.1	60/17	$9 \times 20/51$	II	51/20		1769.8	−1.9
51	1823.9	28	24/7	$16 \times 3/14$	I	14/3	1821.8		2.1
52	[a]1868.0	18	10/3	$9 \times 10/27$	II	27/10		1873.9	−5.9
53	1894.5	3.4	33/10	$9 \times 11/30$	II	30/11		1892.8	1.7
54	1952.5	6.6	16/5	$16 \times 1/5$	I	5/1	1951.9		0.6

[a]Includes a level $E_n = 1868.3$ keV, $\Gamma_n = 1.1$ keV, given in the original data [19].

TABLE V. ^{64}Ni + n s-wave resonances. $S_n = 6098.0$ keV $= (8/45)G = (1/9 + 1/15)G$, $G = 34301$ keV, $E_{\rm rec} = S_n/8 = 762.2$ keV, $E_n = 762.2(m/l)$ keV.

j	E_n (keV)	$g\Gamma_n$	S_n/E_n	$=S_n/E_n$	m/l	$762(m/l)$ (keV)	δ (keV)
1	14.1	2.9	432/1	$8 \times 54/1$	1/54	14.1	0.0
2	33.3	8.9	184/1	$8 \times 23/1$	1/23	33.1	0.2
3	127.3	1.4	48/1	$8 \times 6/1$	1/6	127.0	0.3
4	146.5	0.08	125/3	$8 \times 125/24$	24/125	146.3	0.2
5	152.6	3.95	40/1	$8 \times 5/1$	1/5	152.4	0.2
6	160.7	0.016	800/21	$8 \times 100/21$	21/100	160.1	0.6
7	174.9	0.47	800/23	$8 \times 100/23$	23/100	175.3	−0.4
8	202.1	0.06	30/1	$8 \times 15/4$	4/15	203.3	−1.2
9	216.4	0.03	480/17	$8 \times 60/17$	17/60	216.0	0.4
10	223.4	0.12	600/22	$8 \times 75/22$	22/75	223.6	−0.2
11	228.3	3.8	80/3	$8 \times 10/3$	3/10	228.7	−0.4
12	265.5	2.2	160/7	$8 \times 20/7$	7/20	266.8	−1.3
13	279.1	0.35	240/11	$8 \times 30/11$	11/30	279.5	−0.4
14	293.4	1.0	560/27	$8 \times 70/27$	27/70	294.0	−0.6
15	303.7	1.5	20/1	$8 \times 5/2$	2/5	304.9	−1.2
16	327.8	0.25	56/3	$8 \times 7/3$	3/7	326.7	1.2
17	334.9	0.5	200/11	$8 \times 25/11$	11/25	335.4	−0.5
18	370.1	0.5	33/2	$8 \times 33/16$	16/33	369.6	0.5
19	382.9	6	16/1	$8 \times 2/1$	1/2	381.1	1.9
20	414.3	8	280/19	$8 \times 35/19$	19/35	413.8	0.5
21	475.5	5.0	64/5	$8 \times 8/5$	5/8	476.4	−0.9
22	514.9	1.0	320/27	$8 \times 40/27$	27/40	514.5	0.4
23	521.0	0.75	200/17	$8 \times 25/17$	17/25	518.3	2.7
24	528.2	10	104/9	$8 \times 13/9$	9/13	527.7	0.5
25	543.4	2.0	56/5	$8 \times 7/5$	5/7	544.4	−1.0
26	567.0	4.0	140/13	$8 \times 35/26$	26/35	566.2	0.8
27	573.9	0.3	32/3	$8 \times 4/3$	3/4	571.7	2.2

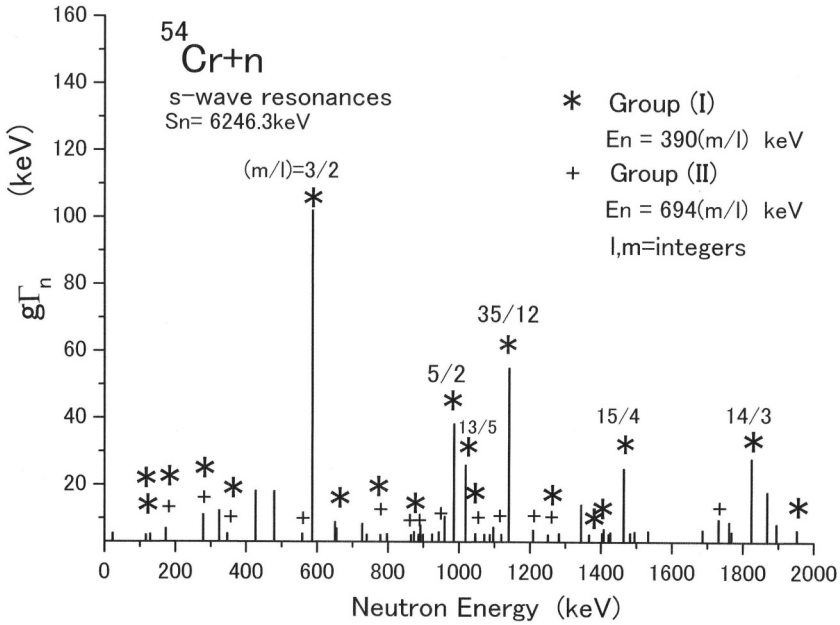

FIG. 3. S-wave resonances of $^{54}\mathrm{Cr}+n$ below 2000 keV. Groups (I) and (II) are shown.

$(l, m \leqslant 10)$ and deviations $|\delta| \leqslant 2.2$ keV. E_n^c can be expressed as

$$E_n^c = \frac{1}{45}\left(\frac{m}{l}\right)G = \frac{1}{8}\left(\frac{m}{l}\right)S_n = 762.2\left(\frac{m}{l}\right)\ \text{keV}, \quad {}^{64}\text{Ni}. \tag{3.17}$$

Numerical data for the probability calculations are summarized in Table II.

H. ^{90}Zr s-wave resonances

The original data are from Musgrove *et al.* [22].

TABLE VI. $^{90}\mathrm{Zr}+n$ s-wave resonances. $S_n = 7194.5$ keV $= (5/24)G = (1/8+1/12)G$, $G = 34533$keV. $E_{\mathrm{rec}} = S_n/40 = 179.8$ keV.

j	E_n (keV)	$g\Gamma_n$ (keV)	S_n/E_n	S_n/E_n	m/l	$180(m/l)$ (keV)	δ (keV)
1	3.8	0.011					
2	13.2	0.065	6000/11	$40\times150/11$	11/150	13.2	0.0
3	17.1	0.20	840/2	$40\times21/2$	2/21	17.1	0.0
4	35.0	0.04	1440/7	$40\times36/7$	7/36	35.0	0.0
5	41.8	0.25	520/3	$40\times13/3$	3/13	41.5	0.3
6	52.8	0.02	1500/11	$40\times75/22$	22/75	52.7	0.1
7	57.5	0.2	500/4	$40\times25/8$	8/25	57.5	0.0
8	70.1	0.23	720/7	$40\times18/7$	7/18	69.9	0.2
9	72.5	0.15	100/1	$40\times5/2$	2/5	71.9	0.6
10	84.8	0.01	600/7	$40\times15/7$	7/15	83.9	0.9
11	89.4	0.02	80/1	$40\times2/1$	1/2	89.9	−0.5
12	112.8	0.14	64/1	$40\times8/5$	5/8	112.4	0.4
13	128.2	0.14	56/1	$40\times7/5$	5/7	128.5	−0.3
14	142.7	0.32	50/1	$40\times5/4$	4/5	143.8	−1.1
15	149.5	0.23	48/1	$40\times6/5$	5/6	149.9	−0.4
16	157.9	0.05	320/7	$40\times8/7$	7/8	157.3	0.6
17	162.5	0.35	400/9	$40\times10/9$	9/10	161.9	0.6
18	166.9	0.13	130/3	$40\times13/12$	12/13	166.0	0.8
19	183.9	0.05	39/1	$40\times39/40$	40/39	184.4	−0.5
20	190.7	0.09	340/9	$40\times17/18$	18/17	190.4	0.3
21	196.2	0.47	110/3	$40\times11/12$	12/11	196.2	0.0
22	205.8	0.10	35/1	$40\times7/8$	8/7	205.6	0.2
23	220.3	0.35	360/11	$40\times9/11$	11/9	219.8	0.5
24	245.7	0.1	320/11	$40\times8/11$	11/8	247.3	−1.6
25	261.9	0.17	110/4	$40\times11/16$	16/11	261.6	0.3
26	269.7	0.29	80/3	$40\times2/3$	3/2	269.8	−0.1
27	297.6	0.41	24/1	$40\times3/5$	5/3	299.8	−2.2

TABLE VII. ^{208}Pb + n s-wave resonances. $S_n = 3937.3$ keV $= (8/70)G = (1/10 + 1/70)G$, $G = 34444$ keV, $E_{\rm rec} = S_n/8 = 492.1$ keV.

j	E_n (keV)	Γ_n (keV)	S_n/E_n	$=S_n/E_n$	m/l	$492(m/l)$ (keV)	δ (keV)
1	503.5	53	8/1	$8 \times 1/1$	1/1	492.1	11.4
2	883.9	5.5	40/9	$8 \times 5/9$	9/5	885.8	− 1.9
3	992.9	3.9	4/1	$8 \times 1/2$	2/1	984.1	8.8
4	1726.7	60	16/7	$8 \times 2/7$	7/2	1722.2	4.5

Twenty seven s-wave resonances are observed below 300 keV shown in Table VI. For many resonances, the factor 8 appears in S_n/E_n. The neutron separation energy $S_n = 7194.5$ keV is regarded as

$$S_n = 7194.5 \text{ keV} = \frac{5}{24}G = \frac{40}{192}G = \left(\frac{1}{8} + \frac{1}{12}\right)G, \quad G = 34533 \text{ keV}, \quad {}^{90}\text{Zr}. \tag{3.18}$$

Considering the factor 8 in S_n/E_n, we use $E_{\rm rec} = (1/192)G = (1/40)S_n = 179.9$ keV. Eleven s-wave resonances of $(l, m \leqslant 10)$ are seen where (m/l) are 2/5, 1/2, 5/8, 5/7, 4/5, 5/6, 7/8, 9/10, 8/7, 3/2, and 5/3 with deviations $\delta \leqslant 1$ keV except for the 4/5 and 5/3 cases. E_n^c can be expressed as

$$E_n^c = \frac{1}{192}\left(\frac{m}{l}\right)G = \frac{1}{40}\left(\frac{m}{l}\right)S_n = 179.9\left(\frac{m}{l}\right) \text{ keV}, \quad {}^{90}\text{Zr}. \tag{3.19}$$

Parameters of the probability calculations are summarized in Table II.

I. ^{208}Pb s-wave resonances

Resonance parameters were measured by Horen *et al.* [23] for 64 resonances of mixed J^π below $E_n < 1$ MeV. For large resonances, Fowler *et al.* [24] reported parameters up to 1.87 MeV. As this nucleus is important (because it is doubly magic) in nuclear physics, we analyze four s-wave resonances below 1.8 MeV as shown in Table VII. In S_n/E_n, the factor 8 appears for all resonances. The separation energy $S_n = 3937.3$ keV is decomposed as

$$S_n = 3937.3 \text{ keV} = \frac{8}{70}G = \left(\frac{1}{10} + \frac{1}{70}\right)G, \quad G = 34451 \text{ keV}, \quad {}^{208}\text{Pb}, \tag{3.20}$$

with LCM = 70 and $E_{\rm rec} = G/70 = S_n/8 = 492.1$ keV. The (m/l) of four s-wave resonances are 1/1, 9/5, 2/1, and 7/2 with deviations $|\delta| \leqslant 12$ keV. E_n^c can be expressed as

$$E_n^c = \frac{1}{70}\left(\frac{m}{l}\right)G = \frac{1}{8}\left(\frac{m}{l}\right)S_n = 492.1\left(\frac{m}{l}\right) \text{ keV}, \quad {}^{208}\text{Pb}. \tag{3.21}$$

It should be noted that $E_{\rm rec} = 492.1$ keV for ^{208}Pb is almost equal to that of $E^1_{\rm rec} = 491.9$ keV for ^{40}Ca(I), which is caused by the same LCM = 70 and hass almost the same G as shown in Table VIII. Because of small sample size, the probability calculation is not made.

J. Summary of family structures and probability calculations

1. *Family structures*

As described above, the observed resonance energies of several e-e target nuclei can be written by simple arithmetic statements, $E_{\rm rec}(m/l)$, with small deviations and where $E_{\rm rec}$ can be derived by several methods described in Sec. III B. Resonances are classified into several groups which seem to coexist in the same energy region without repulsion or attraction. Different values of G are possible for different groups. In many cases, S_n/G are simple sums of inverse integers which are proportional to the cycle times of the oscillators exciting the CN. LCM and $E_{\rm rec}$ are defined for each group of resonances. Decompositions of S_n/G into the sum of inverse integers are summarized in Table VIII.

2. *Probability calculations*

The probabilities of appearance of the family structures P_s are estimated on the assumptions described in Sec. III A and are summarized in Table II. The average P_s for seven cases [excluding Cr-54(II)] is 1.3%. We have investigated neutron resonances of about 40 light and magic nuclides. If we assume random level dispositions for all 40 nuclides, the expectation with $P_s = 1.3\%$ is less than 1 nuclide. The probability of

TABLE VIII. Decomposition of S_n/G into sum of inverse integers. $S_n/G = \sum_{j=1}^{M} 1/n_j$. n_1, n_2, n_3, LCM, $E_{\rm rec}$, and G are shown.

Z	Target nucleus	Group	S_n (keV)	S_n/G	n_1	n_2	n_3	LCM	$E_{\rm rec}$ (keV)	G (keV)
20	Ca-40	(I)	8362.7	17/70	7	10		70	491.9	34434
		(II)		39/162	6	18	54	162	214.4	34737
24	Cr-54	(I)	6246.3	16/88	8	22	88	88	390.4	34354
		(II)		9/50	10	25	25	50	694.0	34701
28	Ni-64		6098.0	8/45	9	15		45	762.2	34301
40	Zr-90		7194.5	5/24	8	12		192	179.9	34533
82	Pb-208		3936.5	8/70	10	70		70	492.1	34444

appearance, U, in 4 nuclides out of 40 is calculated by using a binomial distribution assuming $P_s = 0.013$ as

$$U =_{40} C_4(0.013)^4(0.987)^{36} = 2.0 \times 10^{-3}. \quad (3.22)$$

The occurrence of a phenomenon with a very small probability fails to support the hypothesis of random ensembles of the resonance levels and asserts regular family structures based on the breathing model. Though the random ensembles are the substitution of RMT ensembles, this conclusion will not be changed for RMT ensembles.

IV. DISCUSSION

Though rough and unsophisticated, the breathing model of a CN predicts possible resonance energies by simple arithmetic relations. The breathing model is diametrically different from the prevailing compound nuclear models which predict only statistical properties of the fine structure resonances.

There are many open issues for further investigations; some are described below.

A. Chaosity or regularity

As described in the introduction, it is stressed that the knowledge extracted from the observed data strongly depend on the methods of analysis, as is seen in every field of science. On neutron resonances, the discussions on the chaosity or regularity will be reduced to the different methods of analysis used. By using ordinary methods much of observed neutron resonance data seem to agree well with the predictions of RMT and support the basic assumptions of RMT: randomness or ignorance of the CN.

On the other hand, by using D_{ij} distributions, Fourier-like analyses, and family structures, nonrandom regular structures hidden in neutron resonances are detected from which detailed properties of the compound nuclear system may be read out relating to the breathing model.

B. Regular systems

Neutron resonances of the above nuclei are shown to be regular systems, not chaotic systems. Resonance energies obey simple arithmetic rules, and the hypothesis of the random level ensemble is rejected at a significance level of $\sim 10^{-3}$. This result will be approximately true for the RMT level ensemble. It is also suggested that arithmetic expressions for resonance energies is a facet of general regularities in neutron resonance reactions. The regular family structures described above are the most simple ones, and there will be more and more complex structures in general for which we presently have no methods to detect. We think that similar regularity will survive in low-energy resonances down to the eV region.

C. Meaning of $G \approx 34.5$ MeV

As described above, $G \approx 34.5$ MeV plays an essential role in the energy scale which enables construction of simple dynamic structures in resonance reactions. It is very interesting that G here is near the Fermi energy E_F, the maximum energy of a nucleon trapped in the potential of Fermi-gas model:

$$E_F = (P_F^2)/(2m) \approx 33 \text{ MeV}, \quad (4.1)$$

where m is the nucleon mass and P_F is the Fermi momentum of $(9\pi/8)^{1/3}(\hbar/R_0) \approx 250$ MeV/c, and where $R_0 = 1.20 \times 10^{-15}$ m is a nuclear radius parameter. E_F is independent of mass number. Though small numerical disagreements exist, we think that G is the same physical quantity as E_F, and an oscillator of energy G/n in Sec. II means a wave which is excited in an ensemble of nucleons near the Fermi energy. By using $G \sim 34.5$ MeV, we can reconcile separation energies as sums of inverse integers, suggesting excitation of multiple oscillators with recurrence structures. That the G value deviates slightly (within $\sim$1%) for each case may be caused by the particular situation of the participating oscillators perturbed by several interactions in nuclear potentials. It is suggested that not only neutron resonances but general excitation energies will be written as $E_x = (A/B)G$ with dynamic structures where $A$and B are integers.

D. Response time

$\tau_0 \approx 1.20 \times 10^{-22}$s (=36fm/$c$) defined as $2\pi\hbar/G$ is unit time in the CN. The cycle times of the oscillators excited in the CN are quantized by τ_0 with energies G/n. Also, τ_0 is the minimum time to receive a response from interacting neighbors for (quasi)stable states in the nuclear potential. Through several time exchanges of the response with neighbors, the identity (energies, J^π) will be fixed. In contrast, in high-energy collisions where the collision time is shorter than τ_0 and with no response from interacting neighbors, nuclear chaos will ensue and will show continuous cross sections. This situation corresponds to the region above the "Fermi energy."

E. Coalescent phases

The most interesting and difficult problem will be determining the structures of the coalescent phase. At neutron incidence, many oscillators are excited simultaneously in a short time $\sim\Delta_g$ in the beginning, then several ensembles of oscillators are selectively excited by the periodic passing of the wave crest on the CN with a period τ_w. Resonance reactions take place when the resonance condition of Eq. (2.9) is fulfilled. Neutron separation energy is the energy required to excite oscillators, $G\sum_{j=1}^{q}(1/n_j)$. Several oscillator ensemble groups [(I), (II),...] can be excited. An ensemble of q oscillators recurs after recurrence time LCM$(n_1, \ldots, n_q)\tau_0$, where all phases of the oscillators revert to the original ones and interfere with the pass-by component. The time evolution of the CN at resonance is illustrated in Fig. 4.

Crest-crest nonlinear overlap of several waves of penetrating components produce time-periodic scattering centers for the pass-by component of a few τ_0 duration with buildup of a neutron cloud or flare-up on the CN surface that is synchronized with the incident neutron wave at resonances. The spatial and temporal dependence of the coalescent phases

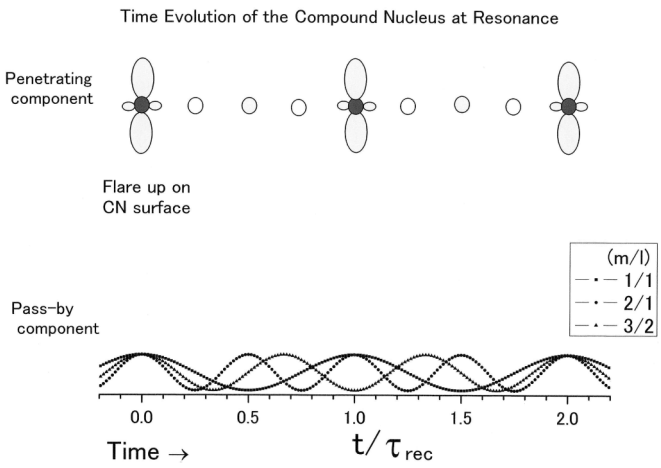

FIG. 4. Time evolution of compound nucleus at resonances. Top: Penetrating component flare-up on the CN surface. Bottom: Pass-by components. Three cases $E_n/E_{\rm rec} = (m/l) = 1/1,\ 2/1$, and $3/2$ are shown.

will be essentially important for nuclear dynamics under strong interactions. Nonlinearity of waves will be enhanced at the nuclear surface due to abrupt changes of potential where higher and lower harmonics and mixing of several frequencies are produced.

The detailed mechanism of breathing of the CN or forming scattering centers on the time axis will be the most interesting problem to be investigated.

F. Recurrence energy $E_{\rm rec}$

The recurrence energy of observed resonances can be deduced by the methods described in Sec. III B. The decompositions of S_n/G into the sum of inverse integers are summarized in Table VI.

For a given S_n, several oscillator ensembles can be excited. Among them, ensembles of the smallest LCM are candidates to be excited because of the minimum recurrence time, analogous to Fermat's principle in optics or Hamilton's principle in mechanics. For the resonances in the keV to eV region, the number of oscillators, q, will be increased and also the number of possible ensembles will be increased. LCM$(n_1, \ldots, n_q)$ will increase to 10^3–10^8.

G. Equidistant level series

In the breathing model, $E_n = 0$ is the special point where the energy scale starts. The angular frequency of the neutron wave, $E_n/\hbar$, is coherent (synchronized) with the recurrence frequency (Poincaré cycle) of the CN at resonances. For incident neutrons off resonance energy, the target nucleus does not respond (stays quiet) and only the potential scattering cross section is observed. By varying the incident neutron energy, the oscillator ensemble will be excited as resonance reactions if the ensemble fulfills Eq. (2.9). In the (m/l) term, equidistant level series appear when $m = 1,\ 2,\ 3, \ldots$ or for integer multiples with the same l value. There will be multiple integer relations among resonance energies and spacings $D_{12} = E_{\rm rec}(m_1/l_1 - m_2/l_2)$ for the same family.

H. Fermi resonance and stroboscope analogy

The family structures described above are a kind of "Fermi resonance" where several frequencies ω_j and integers a_j fulfill the relation

$$\sum_j a_j \omega_j = 0, \tag{4.2}$$

which is caused by nonlinearity of the system. Integer ratios in E_n and $E_{\rm rec}$ in Eq. (2.9b) is the same type,

$$m E_{\rm rec} - l E_n = 0. \tag{4.3}$$

As described in Sec. II E, the stroboscope analogy is also plausible for the physical interpretation of the (m/l) factor. The wave crests of the incident neutron flash up the CN with a time period τ_w. The CN can be imagined as a wheel rotating with a period $\tau_{\rm rec}$. If the ratio between τ_w and $\tau_{\rm rec}$ is a simple integer ratio (m/l), the wheel seems to be stopped under the strobe light. The stop condition of the wheel is equivalent to the possible neutron resonance reactions.

I. Low-energy resonances in the eV region

The number of oscillators (normal modes = degrees of freedom), M, excited in a CN can be estimated by the recurrence time of the classic oscillator ensemble, by assuming a tolerable phase angle error of 1 rad [13] as

$$M = 1 + \frac{\ln(E_x/D)}{\ln(2\pi)}, \tag{4.4}$$

where E_x is the excitation energy and D is the average level spacing. The values of M deduced from observed resonance data are in good agreement with the exciton number n_{ex} of the Fermi gas. For example, when $E_x = 8$ MeV and $D =$ 10eV, the number of excited oscillators will be $M \approx 8.4$. The average energies of these oscillators are $E_x/M \sim 1$ MeV for medium and heavy nuclei with very long recurrence times of $\sim(10^6$–$10^8)\tau_0$. By adding one oscillator, the recurrence time of the CN increases by a factor of $\sim 2\pi$. Integer ratios in $E_{\rm rec}/E_n$ will occur for resonances down to the eV region. However, the methods for searching for $E_{\rm rec}$ described in Sec. III B fail in the eV region, and new methods are needed.

J. Argument against the multistep reaction model

The prevailing reaction mechanism of the CN is the multistep reaction model, in which the initial one-particle zero-hole state (1p-0h) progresses to (2p-1h),. . ., (np-mh) final compound states, leading to internal mixing as a one-way street. The model will be appropriate only for high-energy reactions leading to chaos with continuous energy dependence. Compound nuclei made by multistep reactions are diametrically different from those of the breathing model

for resonance reactions, which are regular systems as described in this article.

V. CONCLUSIONS

Contrary to the premise of quantum chaos, regular structures are found in neutron resonance energies, forming families obeying simple arithmetic relations. For resonances of ^{40}Ca, ^{54}Cr. ^{64}Ni, ^{90}Zr, and ^{208}Pb, family structures are derived where recurrence energies $E_{\rm rec}$ are deduced from S_n/E_n or S_n/G or S_n/LCE. Statistical probability tests strongly support regular family structures for these nuclei. The breathing model of the compound nucleus is developed with the classical analogy of resonance phenomena, from which family structures with arithmetic relations are discerned.

Furthermore, new methods of analysis must be developed to clarify the nonrandom structure of highly excited states of the nucleus. Sophisticated models of nuclear resonance reactions are needed to predict resonance strengths and J^π by drastic refinements of the breathing model. Besides, high-resolution remeasurements and analyses on neutron resonances are required for many nuclei in a wide mass region. Fine structure analyses relating dynamic nuclear models will be an interesting and fruitful area in nuclear physics in the 21st century.

ACKNOWLEDGMENTS

We are deeply indebted to K. Ideno, S. Sukhoruchkin, and Z. Soroko for encouragement of the research in nonstatistical distributions of neutron resonance levels. We also thank S. Sukhoruchkin and Z. Soroko for the very useful edition of their resonance data book [16].

[1] O. Bohigas, R. U. Haq, and A. Pandey, in *Proceedings of the Conference on Nuclear Data for Science and Technology*, edited by K. H. Böchhoff (Reidel, Dordrecht, 1983), p. 809; R. U. Haq, A. Pandey, and O. Bohigas, Phys. Rev. Lett. **48**, 1086 (1982); O. Bohigas, R. U. Haq, and A. Pandey, *ibid.* **54**, 1645 (1985).

[2] T. A. Brody, J. Flores, J. B. French, P. A. Mello, A. Pandy, and S. S. Wong, Rev. Mod. Phys. **53**, 385 (1981).

[3] M. L. Mehta and M. Lal. Mehta, *Random Matrices* (Academic, New York, 2004).

[4] G. E. Mitchell, A. Richter, and H. A. Weidenmuller, Rev. Mod. Phys. **82**, 2845 (2010).

[5] S. Sukhoruchkin, in *Proceedings of the Conference on Nuclear Data for Reactors, Paris, 1966* (IAEA, Vienna, 1967), Vol. 1, p. 159; in *Proceedings of the International Conference on Statistical Properties of Nuclei*, edited by J. B. Garg (Plenum, New York, 1972), p. 215.

[6] K. Ideno and M. Ohkubo, J. Phys. Soc. Jpn. **30**, 620 (1971); K. Ideno, *ibid.* **37**, 581 (1974).

[7] C. Coceva, F. C. Corvi, P. Giacobbe, and M. Stefanon, in *Proceedings of the International Conference on Statistical Properties of Nuclei*, edited by J. B. Garg (Plenum, New York, 1972), p. 447.

[8] F. N. Belyaev and S. P. Borovlev, Yad. Fiz. **27**, 289 (1978) [Sov. J. Nucl. Phys. **27**, 157 (1978)].

[9] S. Sukhoruchkin, *Proc. Int. Seminar on Interaction of Neutrons on Nuclei(ISINN-8)* Dubna 2000, JINR-E3-2000-192; ISINN-7, Dubna 1999, JINR-E3-98-212; ISINN-4, Dubna 1996, JINR -E3-96-336, Z. N. Soroko, S. I. Sukhoruchkin, and D. S. Sukhoruchkin, *ISINN-9*, Dubna-2000, JINR-E-3-2001-192 *ISINN-10*, Dubna-2002, JINR-E-3-2003-10.

[10] S. Sukhoruchkin, Nucl. Phys. A **782**, 37 (2007); *Proceedings of the International Conference on Nuclear Data Science Tecknology, Nice, 2007* (CEA, EDP Sciences, 2008), p. 179; Z. N. Soroko, S. I. Sukhoruchkin, and D. S. Sukhoruchkin, *ISINN-13*, Dubna-2005, JINR-E-3-2006-7 p. 205.

[11] M. Ohkubo, *INDC(JPN)* -185/U, JAERI-Conf 2000-005, p. 325, ibid.-188/U, JAERI-Conf 2001-006, p. 300, ibid.-191/U, JAERI-Conf 2003-006, p. 259.

[12] M. Ohkubo, *J. Nucl. Sci. Technol. Supplement 2, Proc. Int. Conf. ND2001* p. 508 (2002).

[13] M. Ohkubo, Phys. Rev. C **53**, 1325 (1996).

[14] M. Ohkubo, Phys. Rev. C **73**, 054609 (2006).

[15] M. Ohkubo, Phys. Rev. C **80**, 024607 (2009).

[16] Landort Bornstein New Series Group-1 Vol. 24, *Neutron Resonance Parameters*, edited by H. Schopper (Springer-Verlag, Berlin, 2009).

[17] A. G. Sitenko, *Lecture in Scattering Theory* (Pergamon, New York, 1971).

[18] R. Toepke, *KFK-2122*, Karlsruhe (1974).

[19] R. F. Carlton, C. Baker, and J. A. Harvey, Phys. Rev. C **74**, 044614 (2006).

[20] H. Beer and R. R. Spencer, Nucl. Phys. A **240**, 29 (1975).

[21] J. A. Farrell, E. G. Bilbuch, and H. W. Newson, Ann. Phys. (NY) **37**, 367 (1966).

[22] A. R. de L. Musgrove, J. A. Harvey, and W. M. Good, Aust. J. Phys. **30**, 379 (1977).

[23] D. J. Horen, C. H. Johnson, J. L. Fowler, A. D. MacKellar, and B. Castel, Phys. Rev. C **34**, 429 (1986).

[24] J. R. Fowler and E. C. Campbell, Phys. Rev. **127**, 2192 (1962).